有限深抛物势量子盘中极化子的激发态性质

赵翠兰　王丽丽　赵丽丽

Properties of excited state of polaron in quantum disk in finite depth parabolic potential well

Zhao Cui-Lan　Wang Li-Li　Zhao Li-Li

引用信息 Citation: Acta Physica Sinica, **64**, 186301 (2015)　DOI: 10.7498/aps.64.186301
在线阅读 View online: http://dx.doi.org/10.7498/aps.64.186301
当期内容 View table of contents: http://wulixb.iphy.ac.cn/CN/Y2015/V64/I18

有限深抛物势量子盘中极化子的激发态性质*

赵翠兰[1)†] 王丽丽[1)] 赵丽丽[2)]

1) (内蒙古民族大学物理与电子信息学院, 通辽 028043)

2) (赤峰学院计算机与信息工程学院, 赤峰 024000)

(2015 年 3 月 31 日收到; 2015 年 5 月 24 日收到修改稿)

量子点作为一种重要的低维纳米结构, 近年来在单光子光源和新型量子点单光子探测器的研究引起了人们的广泛关注, 对各种势阱中量子点性质的研究已取得了重要成果. 但是大多理论研究都局限于无限深势阱, 而有限深势阱更具有实际意义. 利用平面波展开、幺正变换和变分相结合的方法研究了有限深势阱中极化子激发态能量及激发能随势阱形状和量子盘大小的变化规律. 数值计算结果表明: 极化子的激发态能量、激发能随势垒高度或宽度的增大而增大, 原因是势垒愈高、愈宽, 电子穿透势垒的可能性愈小, 电子在阱内运动的可能性愈大, 进而导致极化子的激发态能量和激发能均随势垒高度和宽度的增大而增大; 极化子的激发态能量和激发能随量子盘半径的增大而减小, 表明量子盘具有显著的量子尺寸效应; 极化子的激发态能量随有效受限长度的增加而减小, 原因是有效受限长度愈大, 有效受限强度愈小, 电子受到的束缚愈弱、振动愈慢、势能愈小, 进而导致基态能量、激发态能量减小; 同时由于激发态能量较基态能量减小慢, 使得激发能随之增加. 研究结果对量子点的应用具有一定的理论指导意义.

关键词: 极化子, 量子盘, 有限深势阱, 激发态

PACS: 63.20.kd, 71.38.–k **DOI:** 10.7498/aps.64.186301

1 引　言

量子点作为一种重要的低维纳米结构, 近年来在单光子光源和新型量子点单光子探测器的研究引起了人们的广泛关注[1,2]. 许多学者对量子点的性质进行了研究, 并取得了重要的成果. 如周青春和狄尊燕[3] 研究了量子点中电子-声子耦合对辐射场相位的影响. Li 和 Xia[4] 用有效质量包络函数理论研究了 InAs/GaAs 量子环的电子态; Chen 等[5] 用 Landau-Pekar 变分法研究了量子阱中极化子的基态性质; Thilagam 和 Lohe[6] 用 Lee-Low-Pines (LLP) 变分法研究了量子阱中相干态极化子的性质; 李亚利和肖景林[7] 用元激发方法研究了无限深量子阱中强耦合极化子的基态结合能; 简荣华和赵翠兰[8] 用相同方法研究了量子阱中弱耦合磁极化子的性质; Filikhin 等[9,10] 在能量依赖有效质量近似下用有限元方法研究量子环的电子态, 并分析了量子环形状和尺寸对电子能态和有效质量的影响; Chang 和 Xia[11] 采用有效质量包罗函数理论, 研究了量子点量子阱结构中电子的性质和光学性质; Chang 和 Lou[12] 还研究了具有反转能带结构的 HgTe 异质结中的量子点的性质; Fang 等[13] 实验研究了 MnS/ZnS 球壳量子点的光致发光温度依赖性; Bagheri 等[14] 利用 Keldysh 非平衡格林函数理论形式以及把电子-声子相互作用多体问题映射为一个单体问题, 研究了串联耦合双量子点分子的性质; Kruchinin 等[15] 建立了一种关于两个球形量子点分子低温稳定光致发光理论, 并对光致发光进行了研究; Liu 等[16] 实验研究了腔耦合量子点的光子发射; Samavatia 等[17] 用实验方法研究热退火对 Si (100) 上射频磁控溅射自组装 Ge 量子

* 国家自然科学基金 (批准号: 11464034) 和内蒙古高校科研基金 (批准号: NJzy13174) 资助的课题.

† 通信作者. E-mail: nmdzcl@163.com

 http://wulixb.iphy.ac.cn

点结构和光学特性的影响.

但是大多数理论研究都局限于无限深势阱, 而有限深势阱更具有实际意义. 本文采用平面波展开、幺正变换和变分相结合的方法研究有限深抛物势阱里量子盘中极化子的激发态性质.

2 理论计算

设半径为 R 的量子盘置于其他介质中, 电子可在盘内外运动, 介质对量子盘中电子的作用等效为一个高度为 V_1、宽度为 d 的势垒. 在有效质量近似下, 电子-声子体系的哈密顿量为

$$H = -\frac{\hbar^2}{2\mu}\nabla_\rho^2 + V(\boldsymbol{\rho}) + \sum_q \hbar\omega_{\mathrm{LO}} a_q^+ a_q + \sum_q \left[V_q a_q \mathrm{e}^{\mathrm{i}\boldsymbol{q}\cdot\boldsymbol{r}} + V_q^* a_q^+ \mathrm{e}^{-\mathrm{i}\boldsymbol{q}\cdot\boldsymbol{r}}\right], \tag{1}$$

其中

$$V_q = \mathrm{i}\left(\frac{\hbar\omega_{\mathrm{LO}}}{q}\right)\left(\frac{\hbar}{2\mu\omega_{\mathrm{LO}}}\right)^{\frac{1}{4}}\left(\frac{4\pi\alpha}{V}\right)^{1/2}, \tag{2}$$

$$\alpha = \left(\frac{e^2}{2\hbar\omega_{\mathrm{LO}}}\right)\left(\frac{2\mu\omega_{\mathrm{LO}}}{\hbar}\right)^{1/2}\left(\frac{1}{\varepsilon_\infty} - \frac{1}{\varepsilon_0}\right), \tag{3}$$

μ 为电子的带质量, ω_{LO} 为光学声子的频率, ρ 为二维坐标矢量, $a_q^+(a_q)$ 是波矢为 $q(q = q_{//}, q_\perp)$ 的体纵光学声子的产生 (湮没) 算符, $\boldsymbol{r} = (\boldsymbol{\rho}, z)$ 为电子的坐标矢量, α 为耦合常数. 电子受到有限深抛物势的作用

$$V(\boldsymbol{\rho}) = \begin{cases} \dfrac{1}{2}\mu\omega^2\rho^2, & 0 \leqslant \rho \leqslant R, \\ V_1, & \rho > R, \end{cases} \tag{4}$$

即盘内受到抛物势的作用, 盘外是高度为 V_1 的势垒, ω 是抛物势的频率, $\omega = \hbar/\mu l^2$, l 是盘型量子阱的有效受限长度.

将势函数 $V(\boldsymbol{\rho})$ 进行偶拓展展开

$$\begin{aligned} V(\boldsymbol{\rho}) = {} & \frac{\mu\omega^2R^3 + 6V_1 d}{6(R+d)} + \frac{\mu\omega^2R^2 - 2V_1}{\pi} \\ & \times \sum_{n=1}^{\infty}\frac{1}{n}\sin\left(\frac{n\pi R}{R+d}\right)\cos\left(\frac{n\pi\rho}{R+d}\right) \\ & + \frac{2\mu\omega^2(R+d)R}{\pi^2}\sum_{n=1}^{\infty}\frac{1}{n^2}\cos\left(\frac{n\pi R}{R+d}\right) \\ & \times\cos\left(\frac{n\pi\rho}{R+d}\right) - \frac{2\mu\omega^2(R+d)^2}{\pi^3} \\ & \times\sum_{n=1}^{\infty}\frac{1}{n^3}\sin\left(\frac{n\pi R}{R+d}\right)\cos\left(\frac{n\pi\rho}{R+d}\right), \end{aligned} \tag{5}$$

其中 d 为势垒宽度.

对哈密顿量 (1) 进行 LLP 幺正变换

$$U = \exp\left[\sum_q \left(f_q a_q^+ - f_q^* a_q\right)\right], \tag{6}$$

其中 $f_q\ (f_q^*)$ 为变分参量, 经过理论计算, 得

$$\begin{aligned} H' = {} & U^{-1}HU \\ = {} & -\frac{\hbar^2}{2\mu}\nabla_\rho^2 + V(\boldsymbol{\rho}) + \sum_q \hbar\omega_{\mathrm{LO}}(a_q^+ + f_q^*)(a_q + f_q) \\ & + \sum_q [V_q^*(a_q^+ + f_q^*)\mathrm{e}^{-\mathrm{i}\boldsymbol{q}\cdot\boldsymbol{r}} + V_q(a_q + f_q)\mathrm{e}^{\mathrm{i}\boldsymbol{q}\cdot\boldsymbol{r}}]. \end{aligned} \tag{7}$$

选取 xoy 平面内电子基态和第一激发态尝试波函数分别为

$$\phi_0(\boldsymbol{\rho}) = \begin{cases} A_1\lambda\,\mathrm{e}^{-\frac{\lambda^2}{2}\rho^2}, & 0 \leqslant \rho \leqslant R, \\ A_1\lambda R\,\mathrm{e}^{\beta R - \frac{\lambda^2}{2}R^2}\dfrac{1}{\rho}\mathrm{e}^{-\beta\rho}, & \rho > R, \end{cases} \tag{8}$$

$$\phi_1(\boldsymbol{\rho}) = \begin{cases} \dfrac{\left[\pi A_1^3\lambda^2 R\,\mathrm{e}^{-R^2\lambda^2} - \dfrac{A_1^3\lambda\pi^{3/2}}{2}\mathrm{erf}(\lambda R) + A_1\lambda^2\rho\right]\mathrm{e}^{-\frac{\lambda^2\rho^2}{2}}}{2\pi(B_1 + B_2)}, & 0 \leqslant \rho \leqslant R, \\ \dfrac{1}{2\pi(B_1+B_2)}\left\{A_1\lambda\beta R\,\mathrm{e}^{\beta R - \frac{\lambda^2R^2}{2}}\dfrac{(1+\beta\rho)\,\mathrm{e}^{-\beta\rho}}{(\beta\rho)^2}\right. \\ \left. -2\pi A_1^3\lambda^3R^2\,\mathrm{e}^{3\beta R - \frac{3\lambda^2R^2}{2}}[\mathrm{e}^{-2\beta R} - \beta R\Gamma(0, 2\beta R)]\dfrac{\mathrm{e}^{-\beta\rho}}{\beta\rho}\right\}, & \rho > R, \end{cases} \tag{9}$$

其中 $\Gamma(0, 2\beta R)$ 是伽玛函数, λ, β 是变分参量, A_1, B_1, B_2 是保证 $\varphi_0(\boldsymbol{\rho})$, $\varphi_1(\boldsymbol{\rho})$ 正交归一的积分常数, 分别为

$$\begin{aligned} A_1 = {} & [\pi(\mathrm{e}^{-\lambda^2R^2} - 1) + 2\pi\lambda^2R^2\,\mathrm{e}^{2\beta R - \lambda^2R^2} \\ & \times\left[\Gamma(0, 2\beta R) - \log\beta - \log(\beta R)\right]^{-\frac{1}{2}}, \end{aligned} \tag{10}$$

$$\beta = \lambda^2 R - \frac{1}{R}, \tag{11}$$

$$\begin{aligned}B_1 = {} & \frac{\pi^2 A_1^6 (1 - \mathrm{e}^{-\lambda^2 R^2})}{2} \\ & \times \left[\lambda R\,\mathrm{e}^{-\lambda^2 R^2} - \frac{\sqrt{\pi}}{2}\mathrm{erf}(\lambda R)\right]^2 \\ & + \frac{A_1^2 [1 - \mathrm{e}^{-\lambda^2 R^2}(1 + \lambda^2 R^2)]}{2} \\ & - \frac{\pi A_1^4}{4} [2\lambda R\,\mathrm{e}^{-\lambda^2 R^2} - \sqrt{\pi}\mathrm{erf}(\lambda R)]^2,\end{aligned} \tag{12}$$

$$\begin{aligned}B_2 = {} & \frac{(\lambda A_1)^2\,\mathrm{e}^{2\beta R - \lambda^2 R^2}}{2\beta^2} [(1 + 2\beta R)\,\mathrm{e}^{-2\beta R} \\ & - 2\beta^2 R^2 \Gamma(0, 2\beta R)] \\ & + \frac{(2\pi A_1^3 \lambda^3 R^2)^2\,\mathrm{e}^{6\beta R - 3\lambda^2 R^2}}{\beta^2} \\ & \times \left[\mathrm{e}^{-2\beta R} - \beta R \Gamma(0, 2\beta R)\right]^2 \\ & \times [\Gamma(0, 2\beta R) - \log(\beta) + \log(\beta R)] \\ & - \frac{4\pi A_1^4 \lambda^4 R^2\,\mathrm{e}^{4\beta R - 2\lambda^2 R^2}}{\beta^2} \\ & \times \left[\mathrm{e}^{-2\beta R} - \beta R \Gamma(0, 2\beta R)\right]^2,\end{aligned} \tag{13}$$

其中 $\mathrm{erf}(x)$ 是误差函数,

$$\mathrm{erf}(x) = \frac{2}{\sqrt{\pi}}\,\mathrm{e}^{-x^2} \sum_{k=0}^{\infty} \frac{2^k x^{2k+1}}{(2k+1)!!}.$$

电子-声子体系的基态尝试波函数选为

$$\Psi_0 = |\phi_{\text{e-p}}\rangle_0 = \phi_0(\boldsymbol{\rho})\,|\xi(z)\rangle\,|0_{\mathrm{ph}}\rangle, \tag{14}$$

其中 $|\xi(z)\rangle$ 是描述电子 z 方向运动的波函数, 因为电子在 z 方向强受限, 所以可以将电子看成只在无限薄的狭层 xoy 平面中运动, 则 $\langle\phi_0(\boldsymbol{\rho})|\phi_0(\boldsymbol{\rho})\rangle = 1$, $\langle\xi(z)|\xi(z)\rangle = \delta(z)$. $|0_{\mathrm{ph}}\rangle$ 为无微扰零声子态, $b_q|0_q\rangle = 0$. 经变分计算, 进一步化简, 取极化子单位 $2\mu = \hbar = \omega_{\mathrm{LO}} = 1$ 后, 得极化子基态能量为

$$\begin{aligned}E_0 = {} & \langle\Psi_0|\,H'\,|\Psi_0\rangle \\ = {} & -2\pi\left\{-\frac{A_1^2\lambda^4 R^2}{2}\,\mathrm{e}^{-\lambda^2 R^2} + A_1^2 \lambda^2 R^2\,\mathrm{e}^{2\beta R - \lambda^2 R^2}\right. \\ & \left.\times \left[\frac{\mathrm{e}^{-2\beta R}}{R^2} + \beta^2 \Gamma(0, 2\beta R)\right]\right\} \\ & + \frac{\omega^2 R^3 + 12 V_1 d}{12(R+d)} \\ & + \left\{\sum_{n=1}^{\infty}\left[\frac{\omega^2 R^2 - 4V_1}{2n\pi}\sin\left(\frac{n\pi R}{R+d}\right)\right.\right. \\ & + \frac{\omega^2 (R+d) R}{n^2\pi^2}\cos\left(\frac{n\pi R}{R+d}\right) \\ & \left.\left.- \frac{\omega^2 (R+d)^2}{n^3\pi^3}\sin(\frac{n\pi R}{R+d})\right]\right\} \\ & \times \left[2\pi A_1^2 \lambda^2 \int_0^R \mathrm{e}^{-\lambda^2\rho^2}\rho\cos\left(\frac{n\pi\rho}{R+d}\right)\mathrm{d}\rho\right. \\ & + 2\pi A_1^2 \lambda^2 R^2\,\mathrm{e}^{2\beta R - \lambda^2 R^2} \\ & \left.\times \int_R^{\infty} \frac{1}{\rho}\,\mathrm{e}^{-2\beta\rho}\cos\left(\frac{n\pi\rho}{R+d}\right)\mathrm{d}\rho\right] \\ & - \sum_q |V_q|^2 \Big|\langle\phi_0(\boldsymbol{\rho})\,|\xi(z)\ \big|\,\mathrm{e}^{\mathrm{i}\boldsymbol{q}\cdot\boldsymbol{r}}\big| \\ & \times \phi_0(\boldsymbol{\rho})\,|\xi(z)\rangle\Big|^2,\end{aligned} \tag{15}$$

电子-声子体系的第一激发态波函数选为

$$\Psi_1 = |\phi_{\text{e-p}}\rangle_1 = \phi_1(\boldsymbol{\rho})\xi(z)\,|0_{\mathrm{ph}}\rangle. \tag{16}$$

同理 $\langle\varphi_1(\boldsymbol{\rho})|\,\varphi_1(\boldsymbol{\rho})\rangle = 1$, $\langle\xi(z)|\,\xi(z)\rangle = \delta(z)$, $b_q\,|0_{ph}\rangle = 0$. 且 $\langle\Psi_0\,|\Psi_1\rangle = 0$, $\langle\Psi_1\,|\Psi_1\rangle = 1$. 则同样计算得极化子第一激发态能量为

$$\begin{aligned}E_1 = {} & \langle\Psi_1|\,H'\,|\Psi_1\rangle \\ = {} & -2\pi(C_1 + C_2) + \frac{\omega^2 R^3 + 12 V_1 d}{12(R+d)} \\ & + \sum_{n=1}^{\infty}\left\{\left[\frac{\omega^2 R^2 - 4V_1}{2n\pi}\sin\left(\frac{n\pi R}{R+d}\right)\right.\right. \\ & + \frac{\omega^2 (R+d) R}{n^2\pi^2}\cos\left(\frac{n\pi R}{R+d}\right) \\ & \left.\left.- \frac{\omega^2 (R+d)^2}{n^3\pi^3}\sin\left(\frac{n\pi R}{R+d}\right)\right] \times C_3\right\} \\ & - \sum_q |V_q|^2 \Big|\langle\phi_1(\boldsymbol{\rho})\xi(z)\ \big|\,\mathrm{e}^{\mathrm{i}\boldsymbol{q}\cdot\boldsymbol{r}}\big|\ \phi_1(\boldsymbol{\rho})\xi(z)\rangle\Big|^2,\end{aligned} \tag{17}$$

其中 C_1, C_2, C_3 分别为

$$\begin{aligned}C_1 = {} & \frac{1}{4\pi^2 (B_1 + B_2)^2}\left\{\frac{A_1^2\lambda^2 [1 - (1 + \lambda^2 R^2)\,\mathrm{e}^{-\lambda^2 R^2}]}{2}\left[\pi^2 A_1^4 \left(\lambda R\,\mathrm{e}^{-\lambda^2 R^2} - \frac{\sqrt{\pi}}{2}\mathrm{erf}(\lambda R)\right)^2 - 3\right]\right. \\ & + \frac{\pi A_1^4 \lambda^2}{8} [2\lambda R\,\mathrm{e}^{-\lambda^2 R^2} - \sqrt{\pi}\mathrm{erf}(\lambda R)][-2\lambda R(3 + 2\lambda^2 R^2)\,\mathrm{e}^{-\lambda^2 R^2} + 3\sqrt{\pi}\mathrm{erf}(\lambda R)] + \frac{\pi A_1^4 \lambda^2}{4} \\ & \left.\times [2\lambda R\,\mathrm{e}^{-\lambda^2 R^2} - \sqrt{\pi}\mathrm{erf}(\lambda R)]^2 [2 - \pi A_1^2 (1 - \mathrm{e}^{-\lambda^2 R^2})] + \frac{A_1^2 \lambda^2}{2}[2 - \mathrm{e}^{-\lambda^2 R^2}(\lambda^4 R^4 + 2\lambda^2 R^2 + 2)]\right\},\end{aligned} \tag{18}$$

$$
\begin{aligned}
C_2 = {} & \frac{1}{4\pi^2(B_1+B_2)^2}\bigg\{A_1^2\lambda^2\beta^2R^2\,\mathrm{e}^{2\beta R-\lambda^2R^2}\left[\frac{(2\beta^3R^3+3\beta^2R^2+6\beta R+3)\,\mathrm{e}^{-2\beta R}}{2\beta^4R^4}-\Gamma(0,2\beta R)\right] \\
& -2\pi A_1^4\lambda^4\beta R^3\,\mathrm{e}^{4\beta R-2\lambda^2R^2}[\mathrm{e}^{-2\beta R}-\beta R\Gamma(0,2\beta R)]\left[\frac{(4\beta^2R^2+7\beta R+8)\,\mathrm{e}^{-2\beta R}}{3\beta^3R^3}-\frac{2\Gamma(0,2\beta R)}{3}\right] \\
& +\frac{4\pi^2A_1^6\lambda^6R^2\,\mathrm{e}^{6\beta R-3\lambda^2R^2}}{\beta^3}[\mathrm{e}^{-2\beta R}-\beta R\Gamma(0,2\beta R)]^2[\mathrm{e}^{-2\beta R}+\beta^2R^2\Gamma(0,2\beta R)]\bigg\}, \qquad (19)
\end{aligned}
$$

$$
\begin{aligned}
C_3 = {} & \frac{1}{2\pi(B_1+B_2)^2}\bigg\{\pi^2A_1^6\lambda^2[\lambda R\,\mathrm{e}^{-\lambda^2R^2}-\frac{\sqrt{\pi}}{2}\mathrm{erf}(\lambda R)]^2\int_0^R\rho\exp(-\lambda^2\rho^2)\cos\left(\frac{n\pi\rho}{R+d}\right)\mathrm{d}\rho \\
& +A_1^2\lambda^4\int_0^R\rho^3\exp(-\lambda^2\rho^2)\cos\left(\frac{n\pi\rho}{R+d}\right)\mathrm{d}\rho+\pi A_1^4\lambda^3[2\lambda R\,\mathrm{e}^{-\lambda^2R^2}-\sqrt{\pi}\mathrm{erf}(\lambda R)] \\
& \times\int_0^R\rho^2\exp(-\lambda^2\rho^2)\cos\left(\frac{n\pi\rho}{R+d}\right)\mathrm{d}\rho+A_1^2\lambda^2\beta^2R^2\,\mathrm{e}^{2\beta R-\lambda^2R^2}\int_R^\infty\frac{\rho\,(1+\beta\rho)^2}{(\beta\rho)^4}\exp(-\lambda^2\rho^2) \\
& \times\cos\left(\frac{n\pi\rho}{R+d}\right)\mathrm{d}\rho+4\pi^2A_1^6\lambda^6R^4\,\mathrm{e}^{6\beta R-3\lambda^2R^2}[\mathrm{e}^{-2\beta R}-\beta R\Gamma(0,2\beta R)]^2\int_R^\infty\frac{\rho}{(\beta\rho)^2}\exp(-\lambda^2\rho^2) \\
& \times\cos\left(\frac{n\pi\rho}{R+d}\right)\mathrm{d}\rho-4\pi A_1^4\lambda^4\beta R^3\,\mathrm{e}^{4\beta R-2\lambda^2R^2}[\mathrm{e}^{-2\beta R}-\beta R\Gamma(0,2\beta R)] \\
& \times\int_R^\infty\frac{\rho(1+\beta\rho)}{(\beta\rho)^3}\exp(-\lambda^2\rho^2)\cos\left(\frac{n\pi\rho}{R+d}\right)\mathrm{d}\rho\bigg\}, \qquad (20)
\end{aligned}
$$

激发能为

$$\Delta E = E_1 - E_0. \qquad (21)$$

3　数值计算与结果讨论

为清楚地表明有限深抛物势量子盘中极化子的激发态性质, 取极化子单位进行数值计算, 结果如图1—图5所示.

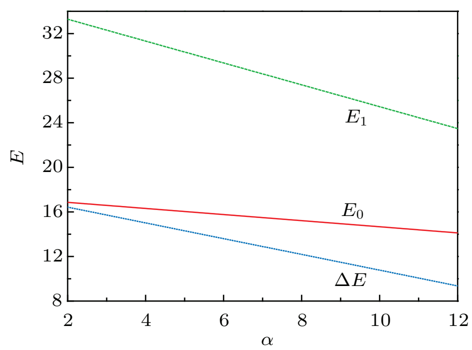

图1　(网刊彩色) 极化子的基态能量 E_0、激发态能量 E_1 和激发能 ΔE 随 α 的变化

Fig. 1. (color online) The correlations between the energy states E_0, E_1, excitation energy ΔE of polaron and α.

图1表示 $R = 0.2$, $d = 0.2$, $V_1 = 25$, $l = 0.2$ 时极化子的基态能量 E_0、第一激发态能量 E_1 及激发能 ΔE 随电子-声子耦合强度 α 的变化关系. 可以看出, 基态能量 E_0、第一激发态能量 E_1 及激发能 ΔE 均随耦合强度 α 的增大而减小, 这是由于耦合强度增大时, 电子和声子之间的相互作用增强, 导致电子和声子相互作用能的绝对值增大, 进而导致极化子的基态能量 E_0、第一激发态能量 E_1 减小. 且由于激发态声子数较多, 电子-声子之间的相互作用较强, 导致其能量较基态下降快, 进而导致激发能减小.

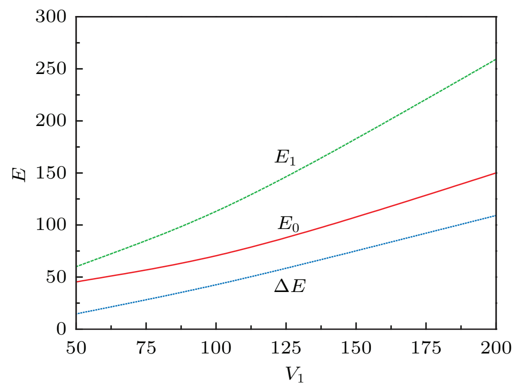

图2　(网刊彩色) 极化子的基态能量 E_0、激发态能量 E_1 和激发能 ΔE 随势垒高度 V_1 的变化

Fig. 2. (color online) The correlations between the energy states E_0, E_1, excitation energy ΔE of polaron and height V_1 of potential barrier.

图2表示 $R = 0.2$, $l = 0.2$, $\alpha = 2$, $d = 0.2$ 时极化子的基态能量 E_0、第一激发态能量 E_1 及激发能 ΔE 随势垒高度 V_1 的变化关系. 可以看出, 基态能量 E_0、第一激发态能量 E_1 及激发能 ΔE 均随势垒高度 V_1 的增高而增大. 图3表示 $R = 0.2$, $l = 0.2$,

$\alpha = 2$, $V_1 = 25$时, 极化子的基态能量E_0、第一激发态能量E_1及激发能ΔE随势垒宽度d的变化关系. 可以看出基态能量E_0、第一激发态能量E_1及激发能ΔE均随势垒宽度d的增大而增大. 这是因为势垒愈高、愈宽, 电子穿透势垒的可能性愈小, 电子在阱内运动的可能性愈大, 电子基态能量及第一激发态能量将增大, 结果导致极化子的基态能量E_0、第一激发态能量E_1及激发能ΔE均随势垒高度和宽度的增大而增大.

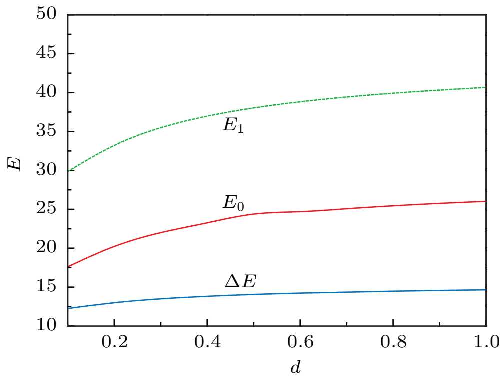

图3　(网刊彩色) 极化子的基态能量E_0、激发态能量E_1和激发能ΔE随势垒宽度d的变化

Fig. 3. (color online) The correlations between the energy states E_0, E_1, excitation energy ΔE of polaron and width d of potential barrier.

图4表示$d = 0.2$, $V_1 = 25$, $\alpha = 2$, $R = 0.2$时, 极化子的基态能量E_0、第一激发态能量E_1及激发能ΔE随有效受限长度l的变化关系. 可以看出基态能量E_0、第一激发态能量E_1随有效受限长度l的增加而减小, 且$l < 0.3$时, 基态能量和第一激发态能量受l的影响比较大, $l > 0.3$时, 受l的影响比较小, 两能量基本趋于不变, 分别达到各自的稳定值. 这是因为有效受限长度l愈大, 有效受限强度愈小, 电子受到的束缚愈弱, 振动愈慢, 势能愈小, 进而导致基态能量E_0和第一激发态能量E_1减小. 当有效受限长度l大到一定程度时, 势能的作用小到可以忽略不计, 则能量不变. 同时可以看到, 激发能ΔE随有效受限长度l的增大而增加, 原因是随着有效受限长度的增大, 激发态的能量变化较基态缓慢, 结果导致激发能增大.

图5表示$d = 0.2$, $V_1 = 25$, $\alpha = 2$, $l = 0.2$时, 极化子的基态能量E_0、第一激发态能量E_1及激发能ΔE随量子盘半径R的变化关系. 可以看出, 基态能量E_0、第一激发态能量E_1及激发能ΔE均随量子盘半径R的增加而减小, 说明量子盘具有明显的量子尺寸效应, 受限愈强, 能量愈大; 同时可见, 激发态的量子尺寸效应较基态显著, 结果导致激发能随半径的增大而减小.

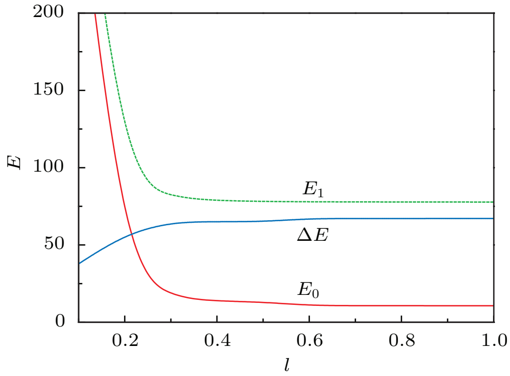

图4　(网刊彩色) 极化子的基态能量E_0、激发态能量E_1和激发能ΔE随有效受限长度l的变化

Fig. 4. (color online) The correlations between the energy states E_0, E_1, excitation energy ΔE of polaron and effective confine length l.

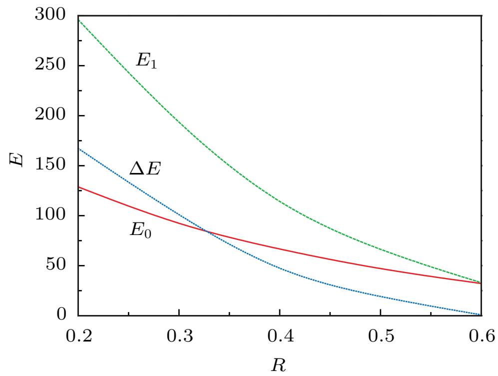

图5　(网刊彩色) 极化子的基态能量E_0、激发态能量E_1和激发能ΔE随半径R的变化

Fig. 5. (color online) The correlations between the energy states E_0, E_1, excitation energy ΔE of polaron and radius R.

4　结　论

利用平面波展开、LLP幺正变换、变分相结合的方法研究量子盘中极化子的激发态性质. 结果表明: 极化子的基态能量、第一激发态能量及激发能均随势垒宽度和高度的增大而增大, 表明势阱形状对极化子的性质有影响. 与文献[18]中无限深势阱结果比较可知, 无限深势阱中极化子激发态能量较有限深势阱中极化子激发态能量下降快. 极化子的基态能量、第一激发态能量及激发能均随耦合强度和量子盘半径的增大而减小. 极化子激发态能量随量子盘有效受限长度的增大而减小, 但激发能与之相反.

参考文献

[1] Wang H Y, Dou X M, Ni H Q, Niu Z C, Sun B Q 2014 *Acta Phys. Sin.* **63** 027801 (in Chinese) [王海艳, 窦秀明, 倪海桥, 牛智川, 孙宝权 2014 物理学报 **63** 027801]

[2] Wang H P, Wang G L, Ni H Q, Xu Y Q, Niu Z C, Gao F Q 2013 *Acta Phys. Sin.* **62** 207303 (in Chinese) [王红培, 王广龙, 倪海桥, 徐应强, 牛智川, 高凤岐 2013 物理学报 **62** 207303]

[3] Zhou Q C, Di Z Y 2013 *Acta Phys. Sin.* **62** 134206 (in Chinese) [周青春, 狄尊燕 2013 物理学报 **62** 134206]

[4] Li S S, Xia J B 2001 *J. Appl. Phys.* **89** 3434

[5] Chen C Y, Lin D L, Jin P W, Zhang S Q, Chen R 1994 *Phys. Rev. B* **49** 13680

[6] Thilagam A, Lohe M A 2005 *Physica E* **25** 625

[7] Li Y L, Xiao J L 2005 *Chin. J. Lumin.* **26** 436 (in Chinese) [李亚利, 肖景林 2005 发光学报 **26** 436]

[8] Jian R H, Zhao C L 2008 *Chin. J. Lumin.* **29** 215 [简荣华, 赵翠兰 2008 发光学报 **29** 215]

[9] Filikhin I, Deyneka E, Vlahovic B 2004 *Modelling Simul. Mater. Sci. Eng.* **12** 1121

[10] Filikhin I, Suslov V M, Vlahovic B 2006 *Physica E* **33** 349

[11] Chang K, Xia J B 1998 *Phys. Rev. B* **57** 9780

[12] Chang K, Lou W K 2011 *Phys. Rev. Lett.* **106** 206802

[13] Fang D F, Ding X, Dai R C, Zhao Z, Wang Z P, Zhang Z M 2014 *Chin. Phys. B* **23** 127804

[14] Bagheri Tagani M, Rahimpour Soleimani H 2014 *Chin. Phys. B* **23** 057302

[15] Kruchinin S Y, Rukhlenko I D, Baimuratov A S, Leonov M Y, Turkov V K, Gun'ko Y K, Baranov A V, Fedorov A V 2015 *J. Appl. Phys.* **117** 014306

[16] Liu Y Y, Petersson K D, Stehlik J, Taylor J M, Petta J R 2014 *Phys. Rev. Lett.* **113** 036801

[17] Samavatia A, Othamana Z, Ghoshalb S K, Mustafac M K 2015 *Chin. Phys. B* **24** 028103

[18] Sarengaowa 2009 *M. S. Thesis* (Tongliao: Inner Mongolia University for Nationalities) (in Chinese) [萨仁高娃 2009 硕士学位论文 (通辽: 内蒙古民族大学)]

Properties of excited state of polaron in quantum disk in finite depth parabolic potential well*

Zhao Cui-Lan[1)†] Wang Li-Li[1)] Zhao Li-Li[2)]

1) (*College of Physics and Electronic Information, Inner Mongolia University for Nationalities, Tongliao 028043, China*)

2) (*College of Computer and information Engineering, Chifeng University, Chifeng 024000, China*)

(Received 31 March 2015; revised manuscript received 24 May 2015)

Abstract

Studies of single quantum state measurement and the relevant physics are very important for the fields of quantum information and quantum coupution. In recent years, quantum dots as information carrier have become a hotpoint of research. The study on quantum dot properties has atracted a lot of attetion and made a series of progress.

In this paper, we formulate a theoretical method that can be used to investigate polaron properties in low-dimensional structures in finite depth potential well. We assume that an electron in a quantum disk which is in other medium is in parabolic potential field, but the effect of the medium on the electron in quantum disk is equivalent to a potential barrier with height V_1 and width d. By expanding the finite height potential barrier as plane waves and Lee-Low-Pines unitary transformation for Hamiltonian, as well as variation for expectation value of Hamiltonian where trial wave functions are obtained by solving the energy eigen-value equation, the ground state energy, the first excited state energy, and excitation energy of polaron are drived.

Numerical calculation by using polaron unit, numerical results indicate that the first excited state energy and excitation energy of polaron increase with increasing the width or height of the potential barrier, because the probability of electron penetrating potential barrier will decrease as the width or height of potential barrier increases, so that electronic energy, the first excited state energy and excitation energy of polaron all increase. Numerical results also show that energies mentioned earlier decrease with increasing radius of quantum disk, which illustrates that the quantum disk has obvious quantum size effect.

It is also found from numerical results that the first excited state energy of polaron decreases with increasing effective confine length, it falls quickly when effective confine length is less than 0.3 and is a little change when effective confine length is more than 0.3. The longer the effective confine length, the more weakly the electron is bounded and the smaller the potential energy is, so that the first excited state energy of polaron decreases. Oppositely, the excitation energy of polaron increases with increasing effective confine length, because the first excited state energy decreases more slowly than the ground state energy.

Keywords: polaron, quantum disk, finite depth potential well, excited state

PACS: 63.20.kd, 71.38.–k **DOI:** 10.7498/aps.64.186301

* Project supported by the National Natural Science Foundation of China (Grant No. 11464034) and the Higher University Science Research Foundation of Inner Mongolia, China (Grant No. NJzy13174).

† Corresponding author. E-mail: nmdzcl@163.com